Correlation properties of a quasiperiodically forced two-level system

Ulrike Feudel, Arkady S. Pikovsky, and Michael A. Zaks
Max-Planck-Arbeitsgruppe "Nichtlineare Dynamik," Universität Potsdam, Potsdam, Germany
(Received 19 July 1994)

We consider a two-level quantum system subject to kicks with a quasiperiodically modulated amplitude. It is shown that, depending on the type of the function that generates the amplitude modulation, two types of spectra can be observed: a discrete one and a singular continuous one. A renormalization group approach is developed for the description of the correlation properties of the system. The two types of spectra are shown to correspond to two fixed points of the renormalization transformation, one in the class of continuous functions and another in the class of discontinuous ones. The crossover between the two types of behavior is investigated numerically.

PACS number(s): 05.45.+b, 03.65.−w, 64.60.Ak

I. INTRODUCTION

The dynamics of quasiperiodically forced quantum systems has attracted considerable interest recently. In the case of a periodic driving force the response can be only quasiperiodic, as follows from the Floquet theorem. An analog of the latter theorem does not exist for quasiperiodic forcing and one may expect more complex types of behavior, maybe even chaos, to be observed in this case. A number of numerical and analytical studies were devoted to this problem. Shepelyansky [1] considered a quasiperiodically kicked rotator system and observed unlimited diffusion of energy, contrary to the periodic case, where the energy growth is limited [2]. Properties of the quasienergy spectrum for this model were studied in Ref. [3], where a transition from the discrete to the continuous spectrum was observed. Pomeau, Dorizzi, and Grammaticos [4] studied numerically a quasiperiodically forced two-level system and observed correlations and spectra typical for chaotic behavior. These results were questioned by Badii and Meier [5], who argued that the conclusions of [4] could be caused by insufficient numerics; see also the discussion by Blekher, Jauslin, and Lebowitz [6]. Sutherland [7] mentioned that slowly decaying correlations may be observed in this system. Then two papers on the quasiperiodically forced two-level system appeared, with apparently contradicting analytical results. Luck, Orland, and Smilansky [8] showed analytically that the two-level system subject to quasiperiodic kicks does not typically have a discrete component in the spectrum, and based on numerical studies they argued that the spectrum is singular continuous. Geisel [9] also showed analytically, for a class of parameter values, that the correlation function of observables in this system was quasiperiodic. He also demonstrated that this quasiperiodicity was very hard to verify numerically and suggested that observations of chaotic-type behavior might be caused by these numerical difficulties. Graham [10] generalized the results of [8] to the N-level case. Combescure [11] showed that the response of the two-level system on a sequence of kicks having a singular continuous spectrum contains in general a discrete and a singular continuous component. Quite recently, Crisanti *et al.* [12] investigated numerically the complexity of a quasiperiodically kicked two-level system; they suggested that its topological entropy is positive. Having all these results, one can conclude that the dynamics of the quasiperiodically driven two-level system still lacks a clear understanding.

In this paper we focus on the correlation properties of the two-level system forced by kicks with quasiperiodically modulated amplitude. Our main result is that the type of the spectrum strongly depends on the form of the external force. In particular, we demonstrate that the two regimes—with a discrete spectrum (as derived by Geisel [9]) and with a singular continuous spectrum (as derived by Luck, Orland, and Smilansky [8])—correspond to continuous and discontinuous modulation functions, respectively. We also perform a renormalization group analysis and demonstrate that the two types of behavior correspond to two fixed points of a renormalization transformation.

The paper is organized as follows. We formulate the basic equations in Sec. II. Then, in Sec. III we analyze two exactly solvable cases for which properties of correlations may be derived analytically. A renormalization group analysis of these cases is described in Sec. IV. We use these findings as a basis for numerical study in Sec. V, where the crossover between the two types of behavior is also discussed.

II. BASIC EQUATIONS

The Hamiltonian describing a two-level system in a time-dependent field $S(t)$ has the form

$$H(t)=\tfrac{1}{2}\omega\sigma_z+\tfrac{1}{2}S(t)\sigma_x ,$$

where σ_x and σ_z are the Pauli matrices

$$\sigma_x=\begin{bmatrix}0 & 1\\ 1 & 0\end{bmatrix},\quad \sigma_z=\begin{bmatrix}1 & 0\\ 0 & -1\end{bmatrix}.$$

The corresponding Schrödinger equation for a spinor (ψ_1,ψ_2) is (it is supposed that $\hbar=1$)

$$i\frac{d\psi_1}{dt}=-\tfrac{1}{2}\omega\psi_1+\tfrac{1}{2}S(t)\psi_2 ,$$
$$i\frac{d\psi_2}{dt}=\tfrac{1}{2}\omega\psi_2+\tfrac{1}{2}S(t)\psi_1 . \quad (1)$$

It is convenient to rewrite this system in terms of the observable Bloch variables

$$A=|\psi_2|^2-|\psi_1|^2 ,$$
$$B=i(\psi_2\psi_1^*-\psi_1\psi_2^*) ,$$
$$C=\psi_2\psi_1^*+\psi_1\psi_2^* ,$$

as

$$\frac{dA}{dt}=S(t)B , \quad (2a)$$
$$\frac{dB}{dt}=-S(t)A-\omega C , \quad (2b)$$
$$\frac{dC}{dt}=\omega B . \quad (2c)$$

Suppose now, following [8,9], that the driving force $S(t)$ is a sequence of δ-function kicks with the basic period T and varying amplitude R:

$$S(t)=\sum_{n=-\infty}^{\infty} R_n\delta(t-nT) . \quad (3)$$

Then between the kicks Eqs. (2) can be solved

$$\tilde{A}=A ,$$
$$\tilde{B}=\cos(\omega T)B-\sin(\omega T)C , \quad (4)$$
$$\tilde{C}=\sin(\omega T)B+\cos(\omega T)C .$$

During the kick only A and B vary; hence

$$\bar{A}=\cos(R)\tilde{A}+\sin(R)\tilde{B} ,$$
$$\bar{B}=-\sin(R)\tilde{A}+\cos(R)\tilde{B} , \quad (5)$$
$$\bar{C}=\tilde{C} .$$

The combination of the two rotations (4) and (5) gives the linear mapping

$$\begin{bmatrix} A_{n+1} \\ B_{n+1} \\ C_{n+1} \end{bmatrix} = \begin{bmatrix} \cos(R_n) & \sin(R_n)\cos(\omega T) & -\sin(R_n)\sin(\omega T) \\ -\sin(R_n) & \cos(R_n)\cos(\omega T) & -\cos(R_n)\sin(\omega T) \\ 0 & \sin(\omega T) & \cos(\omega T) \end{bmatrix} \begin{bmatrix} A_n \\ B_n \\ C_n \end{bmatrix} . \quad (6)$$

Note that the evolution conserves the integral

$$A^2+B^2+C^2=1 . \quad (7)$$

We will further assume that the quasiperiodic sequence R_n is generated by the following dynamical system:

$$\phi_{n+1}=\phi_n+\Omega \pmod 1 , \quad (8)$$
$$R_n=\kappa\Phi(\phi_n), \quad \Phi(\phi+1)=\Phi(\phi) . \quad (9)$$

An irrational Ω in the circle map (8) produces a quasiperiodic sequence ϕ_n and the amplitudes R are defined via the modulation function $\Phi(\phi)$. In Secs. III and IV we will fix Ω to be the reciprocal of the golden mean $\Omega=(\sqrt{5}-1)/2$. The parameter κ defines the level of modulation; we will see below that the properties of the system depend rather subtly on $\Phi(\phi)$ and κ.

Iterations of the mapping (6), (8), and (9) produce the sequences A_n, B_n, and C_n and our goal is to analyze their correlation properties. Mainly, we will use the (normalized) autocorrelation function (it is assumed that $\langle A\rangle=0$)

$$K_A(t)=\frac{\langle A_n A_{n+t}\rangle}{\langle A^2\rangle} \quad (10)$$

(and the corresponding expressions for B_n and C_n). The power spectrum, according to the Wiener-Khinchin theorem, is the Fourier transform of the autocorrelation function. In general, the spectrum may have a discrete (a set of δ-function peaks) and a continuous component. The spectrum of a quasiperiodic function is purely discrete. According to the Wiener theorem (see, e.g., [13]), a necessary and sufficient condition for the spectrum to be purely continuous (no discrete component) is

$$\lim_{N\to\infty} S_N=0 \quad \text{where } S_N=\frac{1}{N}\sum_{t=0}^{N}|K(t)|^2 . \quad (11)$$

A continuous spectrum can have an absolutely continuous component (the spectral measure is equivalent to the Lebesgue measure) and/or a singular component (the spectral measure is singular with respect to the Lebesgue measure). A necessary condition for the spectrum to be absolutely continuous is the decay of the autocorrelation function [13]

$$\lim_{t\to\infty} K(t)=0 . \quad (12)$$

Usually, in dynamical systems the spectra consisting of discrete (periodic or quasiperiodic) and absolutely continuous (chaotic or noisy) components are observed. Recently, singular continuous spectra, which can be viewed as intermediate between quasiperiodic and chaotic, have been reported for a number of physical systems [14–17].

In the next section we consider two special cases for which the nature of the autocorrelation function can be obtained analytically.

III. EXACTLY SOLVABLE CASES

Let us assume that the time interval between δ-function kicks T is a multiple of the basic period $2\pi/\omega$, namely, $\omega T=2\pi m$. In this case, as can be easily seen

from (4), the value of the variable C at the moments of kicks is constant. We can set $C_n=0$ (other choices $C_n<1$ lead only to a renormalization of the variables A_n and B_n). The dynamics then is simply a rotation on the plane (A,B). It is convenient to introduce the phase of this rotation θ_n, so that

$$B_n=\cos\theta_n, \quad A_n=\sin\theta_n \ . \tag{13}$$

The dynamics then reduces to the "skew sum"

$$\phi_{n+1}=\phi_n+\Omega \pmod 1 \ , \tag{14}$$

$$\theta_{n+1}=\theta_n+\kappa\Phi(\phi_n) \ , \tag{15}$$

with the observables defined by (13). Consider now the two choices of the modulation function Φ.

A. Case 1: Continuous modulation function

If we choose, following Geisel [9],

$$\Phi(\phi)=\cos(2\pi\phi) \ ,$$

then the autocorrelation function of $B_n=\cos\theta_n$ can be calculated as follows. First, averaging over the initial phase θ_0 gives

$$\langle B_n B_{n+t}\rangle=\langle\cos\theta_n\cos\theta_{n+t}\rangle=\tfrac{1}{2}\langle\cos(\theta_{n+t}-\theta_n)\rangle \ . \tag{16}$$

Then, using the formula

$$\begin{aligned}\theta_{n+t}-\theta_n&=\kappa\sum_{k=0}^{t-1}\Phi(\phi_{n+k})\\&=\kappa\sum_{k=0}^{t-1}\cos(2\pi\phi_n+k2\pi\Omega)\\&=\kappa\frac{\sin(\pi\Omega t)}{\sin\pi\Omega}\cos[2\pi\phi_n+(t-1)\pi\Omega]\end{aligned} \tag{17}$$

and averaging over the uniform distribution of ϕ_n, we get [9]

$$K_B(t)=J_0\left[\kappa\frac{\sin(\pi\Omega t)}{\sin\pi\Omega}\right] \ , \tag{18}$$

where J_0 is the Bessel function. This autocorrelation function is obviously quasiperiodic (we remind the reader that t is discrete time $t=1,2,\ldots$ and Ω is irrational) and the spectrum is discrete.

B. Case 2: Discontinuous modulation function

Now we choose, similarly to Luck, Orland, and Smilansky [8], the following modulation function Φ:

$$\Phi(\phi)=\begin{cases}2 & \text{if } 0\le\phi<\frac{1}{2}\\ 0 & \text{if } \frac{1}{2}\le\phi<1 \ .\end{cases}$$

Also, we set $\kappa=\pi/2$. Then, θ_n can be either θ_0 or $\theta_0+\pi$, so $A_n=\pm\sin\theta_0$ and $B_n=\pm\cos\theta_0$. From (13) and (15) it follows that we can write a recurrent relation for A and B as

$$D_{n+1}=D_n\cos\left[\frac{\pi}{2}\Phi(\phi_n)\right] \ ,$$

where D stands for A or B. Combining this equation with the circle mapping (14) we get finally

$$\begin{aligned}\phi_{n+1}&=\phi_n+\Omega \pmod 1 \ ,\\ D_{n+1}&=D_n\Theta(\phi_n) \ ,\end{aligned} \tag{19}$$

where

$$\Theta(\phi)=\begin{cases}-1 & \text{if } 0\le\phi<\frac{1}{2}\\ 1 & \text{if } \frac{1}{2}\le\phi<1 \ .\end{cases}$$

Exactly this system was thoroughly studied in mathematical literature. It is called a "skew product" and was introduced by Anzai [18,19]. It was rigorously proven that D has a singular continuous spectrum [20,21,13,22].

Comparing the two cases, we can conclude that the choice of the modulation function Φ is crucial for the correlation properties of the observable variables. We will use these analytical results as a basis for further numerical investigation. We calculate the autocorrelation functions for the cases 1 and 2 numerically and present the results in Figs. 1 and 2. The quasiperiodic autocorrelation function (Fig. 1) has a conventional form with almost exact returns to 1. The autocorrelation function for the process with singular continuous spectrum (Fig. 2) deserves a more detailed description (see also [17]). The following properties can be mentioned.

(i) The values of the autocorrelation function neither return close to 1 nor decay to zero.

(ii) The autocorrelation function looks periodic if the scale of time is logarithmic (this periodicity corresponds, of course, to the regularity of the golden mean; it disap-

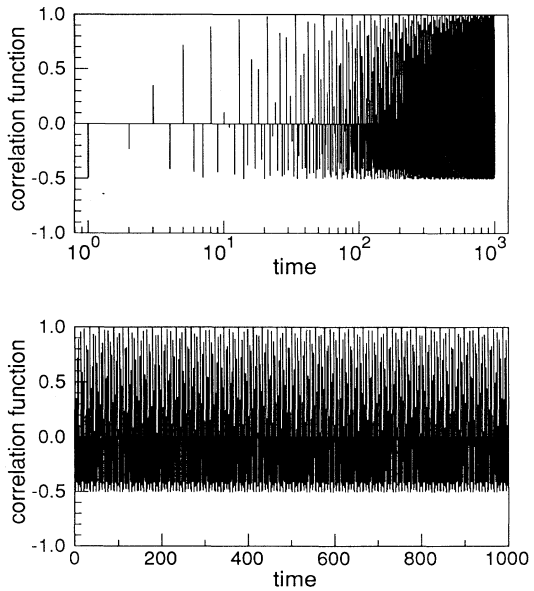

FIG. 1. Autocorrelation function of the observable B for case 1, $\kappa=\pi/2$ (here and below in Figs. 2 and 7: bottom panel, in conventional time scale; upper panel, in logarithmic time scale). This is a typical autocorrelation function of a process with discrete spectrum.

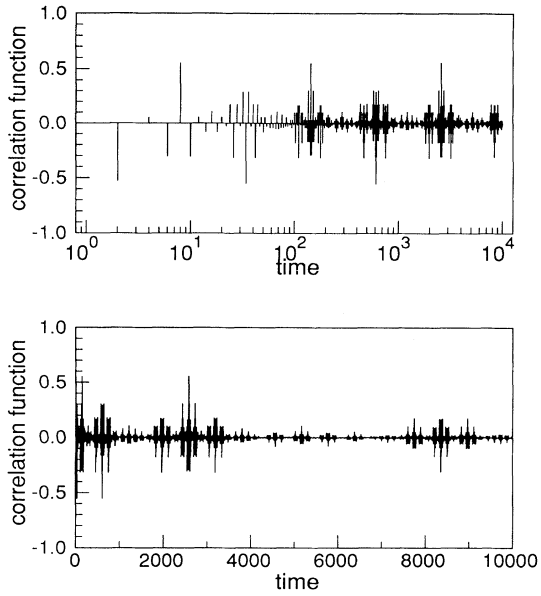

FIG. 2. Autocorrelation function of the observable B for case 2, $\kappa=\pi/2$. This is a typical autocorrelation function of a process with singular continuous spectrum.

pears for a randomly chosen irrational Ω).

(iii) Near each main peak the autocorrelation function reproduces the entire structure, with appropriate scaling. This is clearly seen in Fig. 3, where the part of the correlation function near the peak at $t=2584$ is compared with the part near $t=0$. The explanation of this self-similarity will be given in the next section.

Additionally, we have calculated for these two cases the sum (11). From Fig. 4 one can see that it is indeed

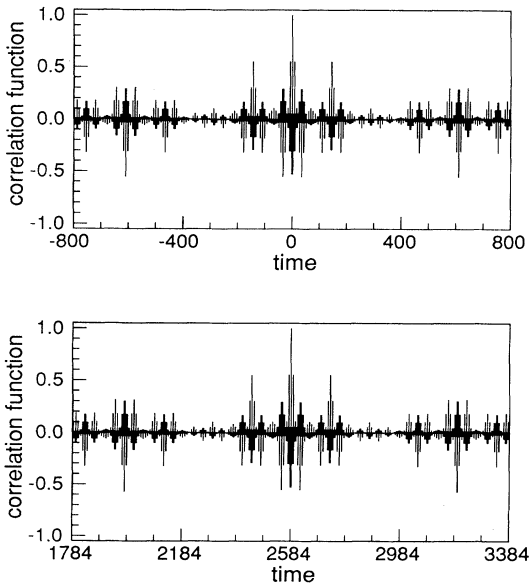

FIG. 3. Self-similar structure of the autocorrelation function Fig. 2. The part near $t=2584$ is magnified, so that $K(2584)=1$, and plotted under the part near $t=0$.

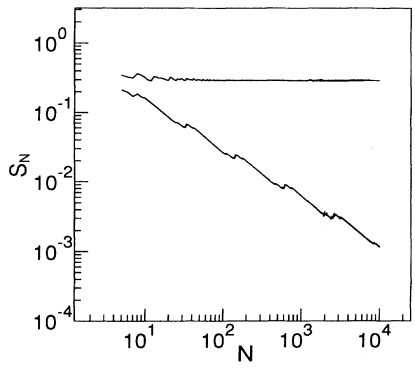

FIG. 4. Sums (11), calculated for the autocorrelation functions in Figs. 1 (upper curve) and 2 (lower curve).

possible to distinguish numerically between the discrete (the sum does not decrease) and the continuous (the sum decreases) spectra. Noting that the correlation function Fig. 2 does not satisfy the necessary condition (12), we conclude that the spectrum is singular.

IV. RENORMALIZATION GROUP

Here we present a renormalization group analysis of the autocorrelation functions described in the preceding section. A similar approach has been developed for strange nonchaotic attractors in Ref. [23].

As one can see from the Eqs. (16) and (17), the autocorrelation function of the observable B can be expressed as

$$K_B(t)=\langle\cos[\kappa Q_t(\phi)]\rangle=\int_0^1\cos[\kappa Q_t(\phi)]d\phi\ , \tag{20}$$

where

$$Q_t(\phi)=\sum_{l=0}^{t-1}\Phi(\phi+l\Omega),\quad Q_0=0\ . \tag{21}$$

Because Ω is the reciprocal golden mean, we expect that the maximum correlations will occur at the "resonant times" of the circle mapping (8) $t=F_m$, where F_m are the Fibonacci numbers ($F_0=0$, $F_1=1$, and $F_m=F_{m-1}+F_{m-2}$). For these times we obtain from (21) a recurrent relation

$$\begin{aligned}Q_{F_m}(\phi)&=\sum_{l=0}^{F_m-1}\Phi(\phi+l\Omega)\\&=\sum_{l=0}^{F_{m-1}-1}\Phi(\phi+l\Omega)\\&\quad+\sum_{l=0}^{F_{m-2}-1}\Phi(\phi+l\Omega+F_{m-1}\Omega)\\&=Q_{F_{m-1}}(\phi)+Q_{F_{m-2}}(\phi+F_{m-1}\Omega)\ .\end{aligned} \tag{22}$$

The phase shift appearing in the last term can be represented as

$$F_{m-1}\Omega=F_{m-2}-(-\Omega)^{m-1} \tag{23}$$

(this is a well-known property of Fibonacci numbers; see

[24,25]). The integer part on the right-hand side of (23) can be omitted [because $Q(\phi)$ is periodic with period 1] and the remaining part suggests that the natural scale of the variable ϕ for the function $Q_{F_m}(\phi)$ is $(-\Omega)^m$. Therefore we introduce a renormalized function as

$$Z_m(y)=Q_{F_m}(y(-\Omega)^m) \tag{24}$$

and obtain from (22) the renormalization transformation

$$Z_m(y)=Z_{m-1}(-y\Omega)+Z_{m-2}(y\Omega^2+\Omega)\ . \tag{25}$$

Although this equation is linear, its dynamics is nontrivial.

Let us take the function $\Phi(\phi)$ in the form $\Phi(\phi)=\exp(i2\pi k\phi)$. Then it follows from (21) that

$$Q_{F_m}(\phi)=\exp(i2\pi k\phi)\frac{1-\exp(i2\pi kF_m\Omega)}{1-\exp(i2\pi k\Omega)}\ . \tag{26}$$

Taking into account the relation (23), we conclude that $|Q_{F_m}|$ tends to zero for any finite k: $|Q_{F_m}|\sim\Omega^m$. This convergence is nonuniform because $|1-\exp(i2\pi k\Omega^m)|=O(1)$ for $k>\Omega^{-m}$. Since the transformations (22) and (25) are linear, we can consider the function $\Phi(\phi)$ to be a superposition of harmonic components and for each of them write (26). The result will depend, however, on the form of the spectrum of $\Phi(\phi)$ due to the nonuniformity mentioned above. If the spectrum decreases sufficiently fast with k (e.g., it consists of one spectral component as in case 1 of Sec. III or decays no slower than k^{-2} as for continuous functions), then the function $Q_{F_m}(\phi)$ decreases with m, which means that the renormalization transformation (25) converges to a trivial fixed point $Z(y)=0$. If the spectrum decreases as k^{-1}, the harmonics with large k dominate in the spectral representation of $Q_{F_m}(\phi)$ and this function does not necessarily decrease with m. This means that the only continuous fixed point of (25) is $Z(y)=0$ [or $Z(y)=$const if we consider modulation functions with nonzero mean value], while there can exist nontrivial discontinuous solutions.

The nontrivial solutions of the renormalization group transformation (25) can be found with the following numerical procedure. We choose the function $\Phi(\phi)$, calculate the sum (21) for $t=F_m$, and then renormalize it according to (24). If we start from a continuous function, e.g., $\Phi(\phi)=\cos(2\pi\phi)$ as in case 1 above, this procedure always leads to the trivial solution $Z(y)=0$. If we start from a discontinuous function, Z does not decay during the iterations. The simplest case is the following choice of the modulation function Φ:

$$\Phi(\phi)=\begin{cases}1 & \text{if } 0\le\phi<\frac{1}{2}\\ -1 & \text{if } \frac{1}{2}\le\phi<1\ .\end{cases} \tag{27}$$

In this case the iterations converge to a period-6 solution of the renormalization transformation (25). We present nonrenormalized functions $Q(\phi)$ in Fig. 5, where the change of a natural scale in ϕ is clearly seen. The rescaled functions Z_m are plotted in Fig. 6.

Having found the solution of the renormalization group equation, it is easy to calculate the autocorrelation function for $t=F_m$, $m\gg1$. Using (20) and (24), we get

$$K_B(F_m)=\langle\cos[\kappa Z_m(y)]\rangle$$
$$=\lim_{L\to\infty}\frac{1}{2L}\int_{-L}^{L}\cos[\kappa Z_m(y)]dy\ . \tag{28}$$

For the continuous fixed point $Z(y)=0$ this gives $K_B(F_m)=1$, while for the discontinuous solution the autocorrelation is less than 1. Consider, e.g., the period-6

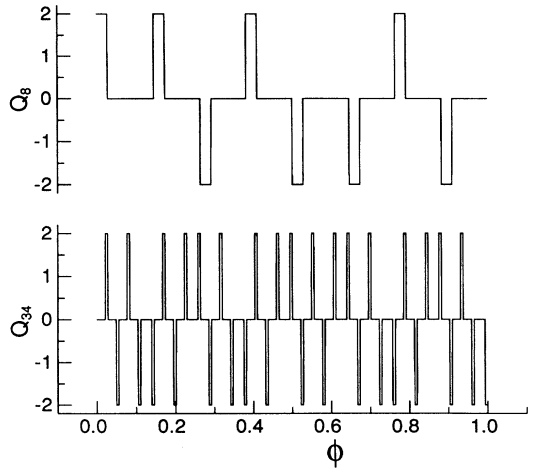

FIG. 5. Nonrenormalized function $Q_{F_m}(\phi)$ for $F_6=8$ and $F_9=34$.

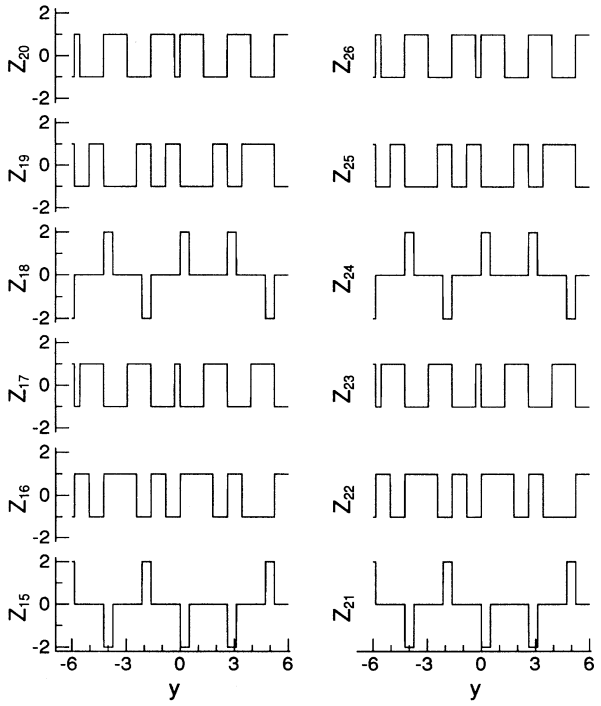

FIG. 6. Period-6 solution of the renormalization transformation (25) with the modulation function (27). We show all the functions for $15\le m\le26$ to make the periodicity clear. Note also the symmetry $Z_{m+3}=-Z_m$.

solution for the function (27), presented in Fig. 6. Here, for $m=3l+1$ and $3l+2$ the function $Z_m(y)$ is ± 1, so for these m the autocorrelation function is $K_B(F_{3l+1})=K_B(F_{3l+2})=\cos(\kappa)$. More complex is the case $m=3l$; here the function $Z_m(y)$ has values $0,\pm 2$ so

$$K_B(F_{3l})=1-a+a\cos(2\kappa)\ ,$$

$$\text{where } a=\tfrac{1}{2}\langle |Z_{3l}| \rangle \approx 0.2236 \quad (29)$$

(the value of a has been obtained numerically from the function Z_{24}). From this representation we see that the case $\kappa=\pi$ is exceptional: here the autocorrelation function returns to 1, like for the continuous modulation function. For other values of the parameter κ the value of K_B at "resonance times" is less than 1 and the minimum is $K_B(F_{3l})=1-2a\approx 0.552\,79$ at $\kappa=\pi/2$. For this value of κ the correlations at $m=3l+1$ and $3l+2$ vanish; the whole autocorrelation function is presented in Fig. 7. It has the same self-similar structure as the autocorrelation function in the exactly solvable case 2 of Sec. III. This self-similarity can be easily understood from our renormalization group approach.

Consider the autocorrelation function at time $F_m \pm t$, where $t \ll F_m$. We can write

$$Q_{F_M \pm t}(\phi)=Q_{F_m}(\phi)\pm Q_t(\phi-(-\Omega)^m)\ ;$$

therefore

$$\begin{aligned} K_B(F_m \pm t) &= \langle \cos[\kappa Q_{F_m}(\phi)]\cos[\kappa Q_t(\phi-(-\Omega)^m)] \rangle \\ &= \int_0^1 d\phi \cos[\kappa Q_{F_m}(\phi)] \\ &\quad \times \cos[\kappa Q_t(\phi-(-\Omega)^m)]\ . \end{aligned}$$

Now we can use that $Q_{F_m}(\phi)$ is a rapidly oscillating function (the characteristic scale is $\Omega^m \approx F_m^{-1}$) without large scale variations [see Fig. 6(b)] and $Q_t(\phi)$ has only large (of order of t^{-1}) scale variations. Thus we can approximate the integral as

$$\begin{aligned} &\int_0^1 d\phi \cos[\kappa Q_{F_m}(\phi)]\cos[\kappa Q_t(\phi-(-\Omega)^m)] \\ &\quad \approx \int_0^1 d\phi \cos[\kappa Q_{F_m}(\phi)] \int_0^1 d\phi \cos[\kappa Q_t(\phi-(-\Omega)^m)] \end{aligned}$$

to obtain

$$K_B(F_m \pm t) \approx K_B(F_m) K_B(t)\ . \quad (30)$$

This formula describes the scaling of the autocorrelation function and explains Figs. 3 and 7. Together with the main resonant times F_m it gives secondary resonances $F_m \pm F_n$, $n<m$, etc. In the continuous case, when at the main resonances the autocorrelation function is close to 1, Eq. (30) shows that at all secondary, third-order, etc. resonances the autocorrelation function is also close to 1; this is clearly seen in Fig. 1. In the discontinuous case this equation gives, for high-order resonant times, a geometrical progression with a factor less than 1 (0.55 for $\kappa=\pi/2$), high-order resonances are small, and main resonant peaks give periodicity in the logarithmic time scale (Fig. 2).

The renormalization approach developed above has some peculiarities in comparison with the usual renormalization group analysis of dynamical systems (see, e.g., [26]). Normally, renormalization is nontrivial only in a critical situation, usually at the border between order and chaos [26]. In our case the renormalization is not attached to any transition, but represents some number-theoretical properties of the irrational Ω. In fact, the scaling obtained for the modulation function (27) represents the regularity of trajectories of points $\phi=0$ and $\frac{1}{2}$ [the coordinates of discontinuities of (27)] in the circle map (8). Another choice of the modulation function will give another scaling, so the properties of the renormalization transformation must very subtly depend on the choice of $\Phi(\phi)$ [13,15,17]. We cannot exclude that some choices of the discontinuous modulation function may lead to a trivial fixed point, thus giving a discrete quasiperiodic spectrum.

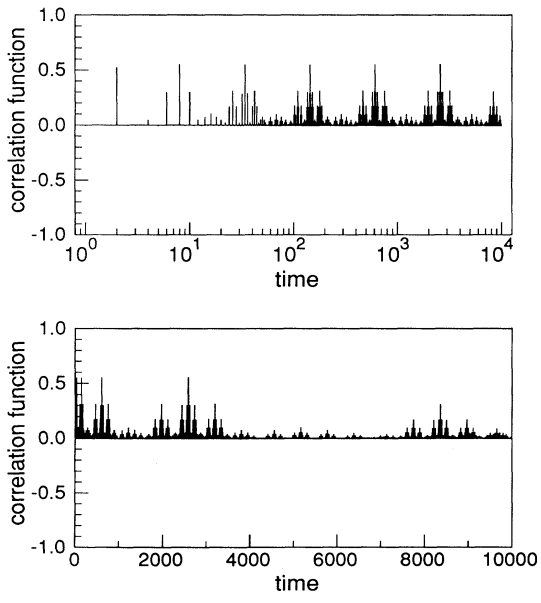

FIG. 7. Autocorrelation function of the observable B in the case of discontinuous modulation function (27) for $\kappa=\pi/2$.

V. NUMERICAL RESULTS

In this section we present results of numerical studies of the cases, which we cannot describe analytically. Our main tool is the calculation of the autocorrelation function and comparison with the patterns of Figs. 1, 2, and 7.

A. Crossover between discrete and singular continuous spectra

The difference in the properties of the autocorrelation function for continuous and discontinuous modulation functions suggests that one can observe a crossover for nearly discontinuous functions. We have checked this for the system (13)–(15) with the modulation function

$$\Phi(\phi)=\begin{cases}\min\{1;(\frac{1}{4}-|\phi-\frac{1}{4}|)\varepsilon^{-1}\} & \text{if } 0\le\phi<\frac{1}{2}\\ \max\{-1;(-\frac{1}{4}+|\phi-\frac{3}{4}|)\varepsilon^{-1}\} & \text{if } \frac{1}{2}\le\phi<1\end{cases}. \quad (31)$$

In this function the vertical segments are replaced by the lines with slope ε^{-1}. The autocorrelation functions obtained for this system for different ε and $\kappa=\pi/2$ are presented in Fig. 8. For small times the correlations are similar to those in the discontinuous case, while for large times the quasiperiodic-type correlations are restored. The crossover is clearly seen in Fig. 9, displaying dependence of the sum (11) on N: after initial decay the sum saturates, which indicates the presence of the discrete component in the spectrum. The saturation level decreases with ε.

B. General case

The whole discussion above was restricted to the case where the main period of the kicks T was a multiple of the period of free rotation $2\pi/\omega$. Now we suppose that both the period of the amplitude modulation and the period of free rotation are incommensurate with the main period and with each other. We chose, following [27,28], the frequency Ω_1 in the circle map (8) and the angle of free rotation $\Omega_2=\omega T/2\pi$ as follows: $\Omega_1=\xi^{-2}$ and $\Omega_2=\xi^{-1}$, where ξ is the so-called "spiral mean"—the real root of $\xi^3-\xi-1=0$; then we iterated the mapping (6) and calculated the autocorrelation function for the observable B. In Fig. 10 we present the results for two

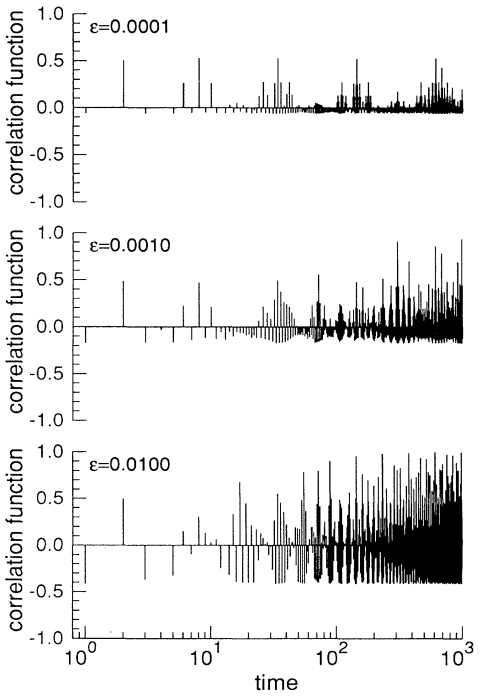

FIG. 8. Autocorrelation functions for the modulation function (31) and different ε. In the limit $\varepsilon\to 0$ the autocorrelation function depicted in Fig. 7 is restored.

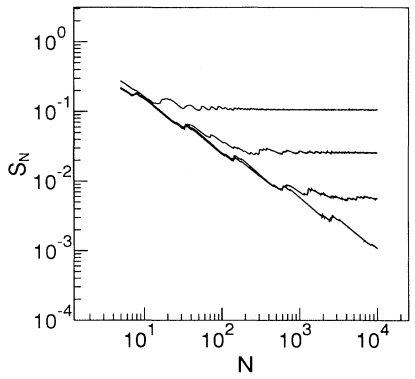

FIG. 9. Sums (11) for the autocorrelation functions in Figs. 8, for $\varepsilon=10^{-2}$, 10^{-3}, 10^{-4}, and 10^{-5} (from top to bottom). The saturation level decreases with ε.

choices of the modulation function Φ: the continuous and the discontinuous. Like in the exactly solvable cases of Sec. III, the difference between the quasiperiodic and the singular continuous spectra is clearly seen in these graphs and in the behavior of the sums (11) (Fig. 11). Thus we can formulate the following hypothesis: if in the quasiperiodically kicked two-level system the modulation function is continuous, a discrete spectrum is observed; if the modulation function is discontinuous, typically a singular continuous spectrum appears.

VI. CONCLUSION

We have shown that the response of the two-level quantum system on the quasiperiodic external forcing

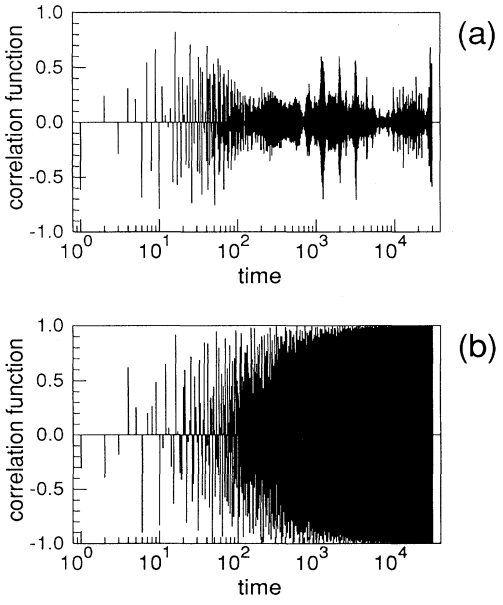

FIG. 10. Autocorrelation functions of the observable B resulted from the general transformation (6) with $\kappa=\pi/8$: (a) discontinuous modulation function (27) and (b) sine modulation function.

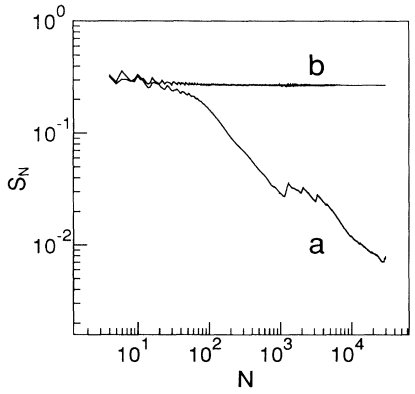

FIG. 11. Sums (11), calculated for the autocorrelation functions in Fig. 10.

strongly depends on the form of the force. If the amplitudes of δ-function kicks are modulated with a continuous function, the spectrum of the observables is discrete; if the modulation function is discontinuous, the spectrum is singular continuous. This resolves the apparent contradiction of the conclusions of Refs. [8] and [9]. These results can be reformulated in the following way. The spectrum of the external force contains all harmonics of the type $n\Omega$ mod 1 (we remind the reader that, because of the discreteness of the process, the spectrum is restricted to the interval [0,1]). For the continuous modulation the harmonics with large n have relatively small amplitudes (e.g., for smooth functions they decay exponentially with n), while for discontinuous modulation they decay only as n^{-1}. This much more dense spectrum of the external force leads to the nontrivial response. It is worth noting that a similar difference has been observed in the studies of spectral properties of the one-dimensional discrete time-independent Schrödinger equation with a quasiperiodic potential. If the potential is given by a cosine function (Harper's equation), a fractal spectrum exists only for one value of the modulation amplitude; if the modulation is discontinuous, the system is critical for arbitrary modulation amplitude [29,16,30,31].

Although throughout this paper we have spoken about spectra, the quantity that was calculated analytically and computed numerically was the autocorrelation function. This function, which is in fact a Fourier transform of the power spectrum, appeared to provide a rather convenient tool to distinguish between different kinds of behavior. The properties of the spectrum itself (e.g., its properties as a multifractal) will be discussed elsewhere.

ACKNOWLEDGMENTS

We thank P. Grassberger, G. Huber, J. Kurths, S. Kuznetsov, G. Mantica, A. Neiman, A. Politi, M. Rosenblum, D. Shepelyansky, U. Smilansky, and A. Vulpiani for useful discussions. M.Z. acknowledges support from the Max-Planck-Gesellschaft.

[1] D. L. Shepelyansky, Physica D **8**, 208 (1983).
[2] B. V. Chirikov, F. M. Izrailev, and D. L. Shepelyansky, Physica D **33**, 77 (1988).
[3] M. Samuelides, R. Fleckinger, L. Touziller, and J. Bellisard, Europhys. Lett. **1**, 203 (1986).
[4] Y. Pomeau, B. Dorizzi, and B. Grammaticos, Phys. Rev. Lett. **56**, 681 (1986).
[5] R. Badii and P. F. Meier, Phys. Rev. Lett. **58**, 1045 (1987).
[6] P. M. Blekher, H. R. Jauslin, and J. L. Lebowitz, J. Stat. Phys. **68**, 271 (1992).
[7] B. Sutherland, Phys. Rev. Lett. **57**, 770 (1986).
[8] J. M. Luck, H. Orland, and U. Smilansky, J. Stat. Phys. **53**, 551 (1988).
[9] T. Geisel, Phys. Rev. A **41**, 2989 (1990).
[10] R. Graham, Europhys. Lett. **8**, 717 (1989).
[11] M. Combescure, J. Stat. Phys. **62**, 779 (1991).
[12] A. Crisanti *et al.*, Phys. Rev. E **50**, 138 (1994).
[13] M. Queffélec, *Substitution Dynamical Systems—Spectral Analysis,* Lecture Notes in Mathematics Vol. 1294 (Springer, Berlin, 1987).
[14] S. Aubry, C. Godrèche, and J. M. Luck, Europhys. Lett. **4**, 639 (1987).
[15] S. Aubry, C. Godrèche, and J. M. Luck, J. Stat. Phys. **51**, 1033 (1988).
[16] R. Artuso *et al.*, Int. J. Mod. Phys. B **8**, 207 (1994).
[17] A. Pikovsky and U. Feudel, J. Phys. A **27**, 5209 (1994).
[18] H. Anzai, Osaka Math. J. **3**, 83 (1951).
[19] In Ref. [21] it is mentioned that this system was first introduced by von Neumann; however, no reference is given.
[20] V. I. Oseledec, Sov. Math. Dokl. **7**, 776 (1966).
[21] A. B. Katok and A. M. Stepin, Russ. Math. Surv. **22**, 77 (1967).
[22] G. W. Riley, J. London Math. Soc. **17**, 152 (1978).
[23] S. Kuznetsov, A. Pikovsky, and U. Feudel (unpublished).
[24] A. Ya. Khinchin, *Continued Fractions* (The University of Chicago Press, Chicago, 1949).
[25] G. H. Hardy and E. M. Wright, *An Introduction to the Theory of Numbers* (Clarendon, Oxford, 1979).
[26] *Universality in Chaos,* edited by P. Cvitanovic (Hilger, Bristol, 1984).
[27] S.-H. Kim and S. Ostlund, Phys. Rev. A **34**, 3426 (1986).
[28] R. Artuso, G. Casati, and D. L. Shepelyansky, Europhys. Lett. **15**, 381 (1991).
[29] D. R. Hofstadter, Phys. Rev. B **14**, 2239 (1976).
[30] M. Kohmoto, L. P. Kadanoff, and C. Tang, Phys. Rev. Lett. **50**, 1870 (1983).
[31] S. Ostlund *et al.*, Phys. Rev. Lett. **50**, 1873 (1983).